Vol. 680: 15–32, 2021
https://doi.org/10.3354/meps13942

MARINE ECOLOGY PROGRESS SERIES
Mar Ecol Prog Ser

Published December 9

Contribution to the Theme Section 'Advancing dynamic modelling of marine populations and ecosystems'

Patterns, efficiency and ecosystem effects when fishing *Calanus finmarchicus* in the Norwegian Sea — using an individual-based model

Cecilie Hansen*, Morten D. Skogen, Kjell Rong Utne, Cecilie Broms, Espen Strand, Solfrid Sætre Hjøllo

Institute of Marine Research, 5817 Bergen, Norway

ABSTRACT: Due to the important role of *Calanus finmarchicus* as key prey for the abundant pelagic fish stocks (Northeast Atlantic mackerel, Norwegian spring spawning herring, blue whiting) in the Norwegian Sea, an increase in the quota of *C. finmarchicus* has raised public concern. Here, 2 vessel types were implemented in an individual-based model within the NORWECOM.E2E ecosystem model, one ordinary vessel similar to the vessels used in the real fishery, the other with perfect knowledge of the *C. finmarchicus* distribution to account for possible future development of the fishery. The perfect vessels were free to move among all grid cells, whereas the other vessel type was restricted. Differences between the vessel types were large in terms of catch per unit effort and hotspots for catches. Operating with 10 perfect vessels, the catches were on average 54 000 t yr^{-1}, almost 3 times higher than for the ordinary vessels. Increasing to 60 perfect vessels, catches increased to 349 000 t yr^{-1}. The vessels with full knowledge of distribution and concentration located new hotspots distant from the traditional fishing grounds. Due to area restrictions in the current quota, allowing only 3000 t caught within the 1000 m depth contour, the perfect vessels shifted their activity offshore. In the simulated ecosystem, no ecosystem effects were found, neither on the *C. finmarchicus* biomass nor on the Norwegian spring spawning herring biomass. This finding indicates that the proposed quota of *C. finmarchicus* supports a sustainable fishery.

KEY WORDS: Individual-based models · Zooplankton · Lower-trophic level harvest · *Calanus* fisheries · NORWECOM.e2e

1. INTRODUCTION

The demand for marine oils from the aquaculture and human health industries is rising (FAO 2020). However, a sufficient annual increase in fisheries catches to produce fishmeal and fish oil is challenging within a conventional harvesting regime, as the majority of the world's fish stocks are fished at or above sustainable levels (FAO 2020). This situation has led to a growing interest in increased harvest of zooplankton. Any significant increase in harvesting lower trophic level organisms will likely cause concern within the fishing community and environmental organizations, as zooplankton constitute the food base for fish stocks. However, fishing the more productive components of the ecosystem has been repeatedly proposed, e.g. in the form of balanced harvesting (e.g. Garcia et al. 2012, Zhou et al. 2019), and a zooplankton fishery could be a strategic move to increase yield of marine resources if done in a sustainable manner (Hansen et al. 2019). Given the interest in an expansion of zooplankton harvesting, knowledge is required on how to assess the existing stocks and the effect such harvest may have on other

*Corresponding author: cecilie.hansen@hi.no

Publisher: Inter-Research · www.int-res.com

parts of the ecosystem — in particular already exploited fish stocks. Exploration of resource dynamics when introducing the human dimension through spatially explicit fisheries calls for integrative methods such as ecosystem modelling, which can explore present and future scenarios and enhance our understanding of a complex reality.

Examples of existing zooplankton fisheries can be found at high latitudes. The krill stock in the Southern Ocean has been harvested for decades, managed by the Commission for the Conservation of Antarctic Marine Living Resources (CCAMLR). Due to economic interest in the ester oil found in *Calanus finmarchicus*, there has been an ongoing trial fishery of *C. finmarchicus* for almost 2 decades in the Norwegian Sea, targeting copepods at stages IV–VI. The given quota has been 1000–5000 t wet weight (WW) yr^{-1}. Recently, a management plan was implemented, increasing the total allowable catch to 254 000 t WW (www.regjeringen.no/no/dokumenter/forskrift-om-regulering-av-hosting-av-rodate-i-2019/id2632216/, accessed 19 October 2021). Of these, 3000 t can be caught in waters shallower than 1000 m off the Norwegian coast. The division of the quota, with a more restricted fishery close to shore, aims to limit unwanted bycatch of fish eggs and larvae.

Calanus finmarchicus is the dominating zooplankton in the Norwegian Sea, with its production closely related to the phytoplankton bloom (Broms & Melle 2007). The annual *C. finmarchicus* production varies but is estimated to be 190–290 million t WW (Melle et al. 2004, Skjoldal et al. 2004, Hjøllo et al. 2012). With a standing stock biomass of close to 30 million t WW, *C. finmarchicus* is an ecologically important species through its role as essential prey for carnivorous and omnivorous zooplankton such as amphipods, krill and chaetognaths and for many species of fish larvae and planktivorous fish (Melle et al. 2004, Skjoldal et al. 2004, Prokopchuk & Sentyabov 2006, Langøy et al. 2012, Utne et al. 2012, Bachiller et al. 2018). The Norwegian Sea is a key feeding area to several commercially important planktivorous fish species including Norwegian spring spawning (NSS) herring *Clupea harengus*, blue whiting *Micromesistius poutassou*, and mackerel *Scomber scombrus*, which enter the Norwegian Sea during summer to utilize the abundant zooplankton resources (Misund et al. 1998, Utne & Huse 2012, Olafsdottir et al. 2019).

The ecological consequences of an increased *C. finmarchicus* fishery are not well known, but impact on the *C. finmarchicus* stock, bycatch of egg and larvae, as well as effects on plankton-feeding fish stocks is important to assess (Broms et al. 2016, Fiskeridirektoratet 2016). The main aim of the present work is to explore resource dynamics when introducing selected scenarios of spatially explicit *C. finmarchicus* fishery in the Norwegian Sea. We present a newly developed individual-based model (IBM) of fishing vessels, combined with a spatially explicit existing end-to-end ecosystem model for the Norwegian and Barents Sea. The fishing vessel IBM is vessel-specific, and 2-way coupled to an existing ecosystem model including individual-based modules for *C. finmarchicus* and for the NSS herring stock. The 2-way coupling between the *C. finmarchicus* resources and the fishing vessels allows for inclusion of adaptive fishing patterns in time and space, and thus exploration of ecosystem effects. As the *C. finmarchicus* fishery is still in its infancy, 2 different types of fishing vessels were implemented; one mimicking the vessels taking part in today's fisheries (termed ordinary vessels), while the other has an intrinsic knowledge of the concentration of *C. finmarchicus* biomass and can target their fishing in a more sophisticated way (termed perfect vessels). Sensitivity testing was performed for relevant parameters. We investigate the effects of the harvest patterns, number of vessels, fishery efficiency and potential ecosystem impact under different ecological conditions for a selected period (1995–1999), with the aim of exploring the sustainability of a *C. finmarchicus* fishery in the Norwegian Sea.

2. METHODS

2.1. NORWECOM.E2E

The NORWegian ECOlogical Model system End-To-End (NORWECOM.E2E) is a merger of a Nutrient-Phytoplankton-Zooplankton-Detritus (NPZD) model for plankton and nutrient cycling (Skogen et al. 1995) and different IBMs developed initially for zooplankton (Hjøllo et al. 2012) and fish (Utne et al. 2012). In the present study, a newly developed IBM for fishing vessels (Section 2.2) is presented and used together with the NPZD and the IBMs for *Calanus finmarchicus* and NSS herring (Fig. 1). Physical ocean fields (velocities, salinity, temperature, water level and sea ice) are taken from a hindcast simulation (Budgell 2005, Lien et al. 2006) using the Regional Ocean Modelling System (ROMS) model (Shchepetkin & McWilliams 2005). The horizontal grid in the model domain (Fig. 2) is identical to a subdomain of the original ROMS grid, with a spatial resolution close to 20 × 20 km.

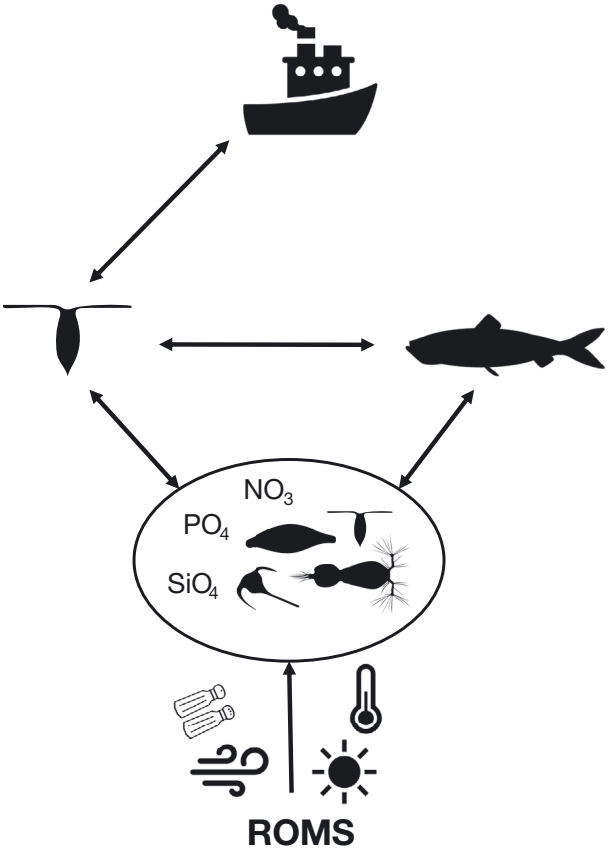

Fig. 1. NORWECOM.E2E model system, including the individual-based models for *C. finmarchicus*, herring and fishing vessels. Forcing from the oceanographic ROMS model is indicated by salt, sun, temperature and current symbols. Arrows indicate direction of forcing or interaction. *C. finmarchicus* preys on diatoms, flagellates and microzooplankton (included in the oval). Herring preys on the *C. finmarchicus* and the mesozooplankton species in the oval. The vessels will catch *C. finmarchicus*, removing them from the total biomass. At the same time, the *C. finmarchicus* distribution will have an impact on where the vessels will travel

The NPZD model is coupled to the physical model through the subsurface light, the hydrography and the horizontal and vertical movement of the water masses, while the IBM for *C. finmarchicus* is 2-way coupled to the NPZD model where it enforces grazing on the phytoplankton and microzooplankton. The IBM addresses the full *C. finmarchicus* 13 stage life cycle, from eggs to spawning adults (eggs + 6 nauplii + 6 copepodites), and considers growth, mortality, movement and reproduction as well as adaptive traits (Huse et al. 2018), which control interaction with the environment. Due to the great abundances involved, *C. finmarchicus* is simulated using the super-individual (SI) approach (Scheffer et al. 1995), in which 1 SI represents many (~10^{12}) identical individuals, and the number of such identical siblings is an attribute of the SI. The traits of each SI are constant, but as offspring inherit their traits from their parents and the population is not reinitialized every year, the traits of the SIs with high fitness will over time change the traits of the population.

When it comes to seasonal/ontogenic vertical migration in *C. finmarchicus*, the actual mechanism(s) triggering it are far from understood. Life history and behavioral strategies of individuals are therefore modelled through a strategy vector (Huse et al. 1999), consisting of 5 behavioral and life-history-adaptive traits: (1) the date for ascent from overwintering to the surface, (2) the day for initiating fat allocation in copepodite stage CV, (3) fat/soma ratio needed before descending to overwinter, (4) overwintering depth and (5) diurnal vertical migration (Huse et al. 2018).

Horizontal movement is due to passive drift using the velocity fields from the ROMS model and a 4th order Runge-Kutta method. The initial distribution field for *C. finmarchicus* is based on an overwintering population of *C. finmarchicus* distributed in the deeper Norwegian Sea basins, on the border between the Norwegian and Greenland Seas and also in the Barents Sea, evolved through a 4-yr-long adaptation process (Hjøllo et al. 2012).

The predation pressure by fish on zooplankton was modelled dynamically by including a full life cycle IBM for NSS herring (Utne et al. 2012). As for the *C. finmarchicus* IBM, the pelagic fish are simulated using the SI approach due to the great number of individuals involved. The pelagic fish feed on *C. finmarchicus* and mesozooplankton from the NPZD model with a 2-way coupling so that consumed plankton is instantaneously removed in the model. In the herring IBM, the fish migration is driven by predefined directional migrations from survey observations and the *C. finmarchicus* densities, mimicking large scale migrations. The use of the herring IBM is intended to lead to a realistic predation pressure on zooplankton by fish in time and space. Individual growth and consumption are handled by a bioenergetic model, in which herring feeding intensity in simulations without a *C. finmarchicus* fishery recreates observed individual growth (Utne et al. 2012).

The *C. finmarchicus* IBM has been validated in previous studies by Hjøllo et al. (2012) in the Norwegian Sea, Dalpadado et al. (2014) and Skaret et al. (2014) in the Barents Sea and Gao et al. (2021) in the North Sea. The NOWECOM.E2E model system is flexible and allows the user to select which modules to include. All modules are 2-way coupled, and changes will introduce non-linear effects, e.g. apply-

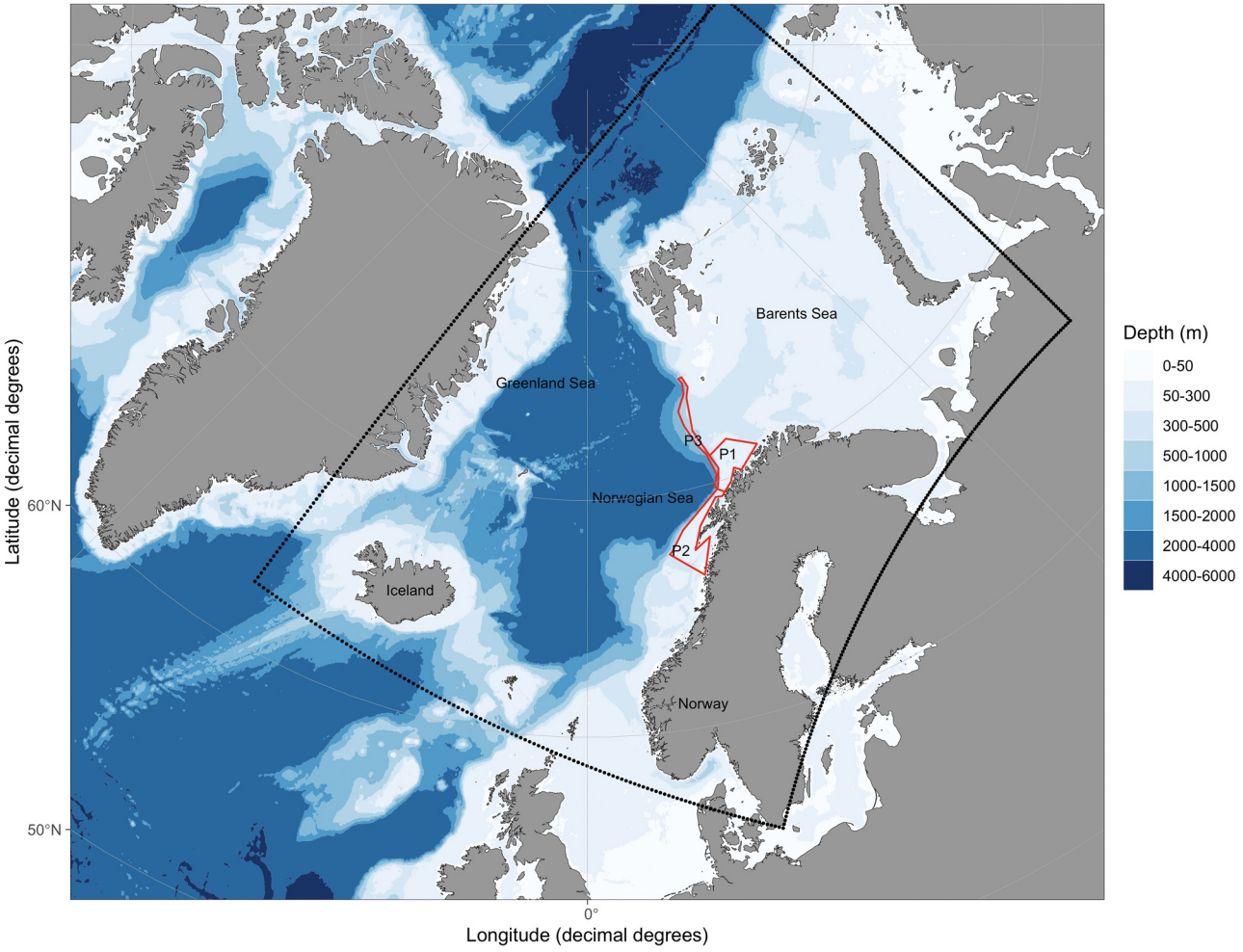

Fig. 2. Model domain of the NORWECOM.E2E model marked with black dots. Depth color: dark blue (deep) to pale blue (shallow). Pale blue areas (depth < 1000 m) are included in the quota restrictions (*C. finmarchicus* catch limit of 3000 t). Red areas: where the local impact of *C. finmarchicus* harvest was evaluated. P1: Lofoten north, P2: Lofoten south, P3: shelf edge. Figure created with R-package ggOceanMaps (Vihtakari 2021)

ing a *C. finmarchicus* fishery by the fishing vessel IBM will influence the *C. finmarchicus* stock, and then subsequently the prey and predators of *C. finmarchicus*.

2.2. New module: the fishing vessel IBM

The description of the fishing vessel IBM follows the Overview, Design concepts and Details protocol (Grimm et al. 2006) to enhance readability and reproducibility of IBMs.

2.2.1. Purpose

The purpose of the module was to explore the movement and catch pattern of fishing vessels which harvest *C. finmarchicus*, and the ecosystem effects of such a fishery. The fishing vessel module is 2-way coupled with the *C. finmarchicus* IBM in the NORWECOM.E2E ecosystem model. The fishing vessels only target the largest individuals, represented by stages CIV, CV and CVI. The fishing vessel module is general and can easily be adapted to perform fisheries on other species in the NORWECOM.E2E model.

2.2.2. State variables and scales

The model included fishing vessels, their movement and properties. The attribute vector included 24 state variables such as catch capacity, position, fuel usage and speed (Table 1). As there were few individual fishing vessels (10 and 60), they could

Table 1. Characteristics of the fishing vessels used in the simulations. NA: not applicable (for unitless values). NOK: Norwegian kroner

Parameter	Type	Value	Unit	Description
Name	Constant	1–10 or 1–60	NA	Vessel name or no.
Position (*x*,*y*,***z***)	Dynamic	Grid cell no.	NA	Position in grid
Trawlspeed	Constant	0.5	m s^{-1}	Speed when trawling
Speed	Constant	3	m s^{-1}	Steaming speed
Maxspeed	Constant	5[a]	m s^{-1}	Maximum speed
Route_empty	Dynamic	True/False	NA	Defines if vessel needs a new route
In_harbor	Dynamic	True/False	NA	Defines if vessel is in harbor
Harbornr	Dynamic	1-10	NA	Home harbor
Resting	Dynamic	True/False	NA	If vessel is resting
Carrcap	Dynamic	0 – maxcarr	kg	Catch capacity left after fishing
Maxcarr	Constant	450000	kg	Maximum catch capacity for each vessel
Fuel	Dynamic	0 – fuelcap	l	Fuel left in vessel
Fuelcap	Constant	40000[a]	l	Maximum fuel capacity
Fuelprice	Constant	8	NOK l^{-1}	Price per l of fuel
Fuelcons	Constant	87[a,b]	l h^{-1}	Fuel consumption per hour
Gearsize	Constant	7	m^2	Horizontal area covered by gear
Geardepth	Constant	5	m	Vertical depth of gear
Nrgears	Constant	2	NA	Number of trawls
Vertfrac	Constant	0.75	NA	Fraction of vertical distribution made available for harvest
Fishlimit	constant	5	g m^{-2}	Level of *C. finmarchicus* initiating fishing
Catch	Dynamic	NA	t	Catch per day
Restt	Dynamic	0–20	d	How long vessel has been resting
Catchprice	Constant	11	NOK kg^{-1}	Assumed price per kg catch
Isperfect	Constant	True/false	NA	If vessel has perfect knowledge about the concentrations
Mypath	Dynamic	Vector of (*x*,*y*)	Grid cell no.	Path to follow
Bestfg	Dynamic	Point (*x*,*y*)	Grid cell no.	Which fishing ground to steam towards
Activity	Dynamic	1	NA	Activity
		2		Resting
		3		Route empty
		4		Full
		5		No fuel
		6		Changing fishing ground
		7		In harbor
		8		Unknown

[a]Value selected based on Bastardie et al. (2010); [b]Fuel consumption was based on horsepower data for the 2 vessels catching *Calanus finmarchicus* (taken from www.kystmagasinet.no/nyheter/fiskeflatens-kraftkarer-2, accessed 19 October 2021) using a conversion based on Bastardie et al. (2010)

each be represented by one modelled individual. The attributes were based on 2 of the most used vessels used for the *C. finmarchicus* fisheries in the Norwegian Sea.

2.2.3. Process overview and scheduling

The processes governing the individuals were the 2 logistic loops, representing an ordinary vessel (Fig. 3a) and a perfect vessel (Fig. 3b). The logistic loop defined in Fig. 3a was to a large degree founded on the logistic loop in Bastardie et al. (2014). The 2-way coupling with the *C. finmarchicus* IBM was through removal of *C. finmarchicus* due to harvesting, and changes in the available *C. finmarchicus* biomass for the vessels due to processes included in the *C. finmarchicus* IBM.

2.2.4. Design concepts

Emergence. Vessel behavior emerged from the logistic loops that decided where they should go and if the vessels should be fishing. Similarly, vessel catch, trip duration, activity (e.g. fishing, steaming) and fuel consumption emerged from the vessel behavior.

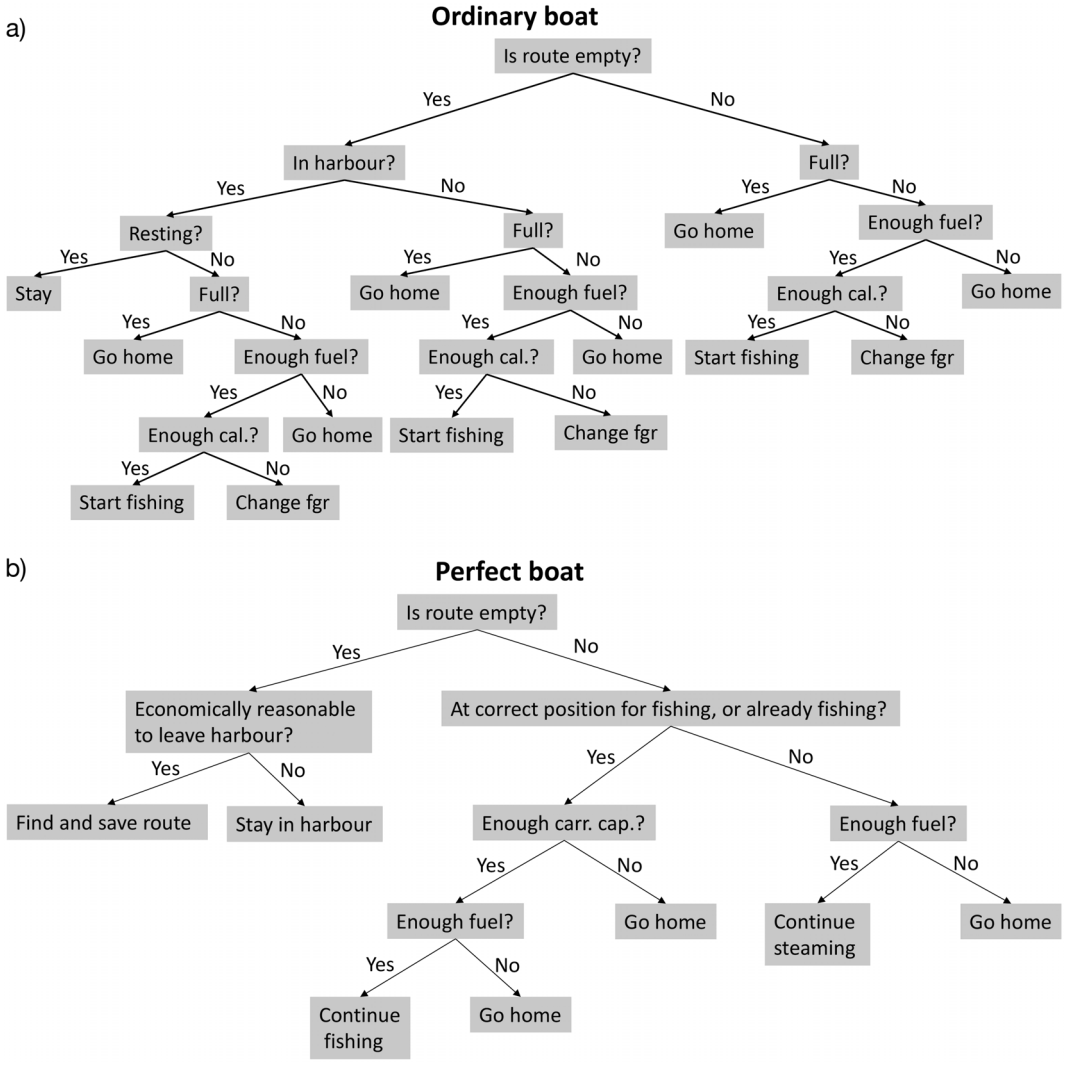

Fig. 3. Logical loop for the (a) ordinary and (b) perfect vessels. Perfect vessels will always return to their home harbor instead of the closest harbor. Cal: amount of *C. finmarchicus* available for harvest; fgr: fishing ground; Full: catch capacity of the vessel was reached, so vessel needs to return to land its catch

Fitness. Fitness could be measured in catch per unit effort, calculated as the catch (in t WW) divided by the time the vessel was actively fishing (in d).

Sensing. The concentration of *C. finmarchicus* in each grid cell was given as input to the fishing vessel module. This was applied to guide the path of the perfect fishing vessels, through Eqs. (2) & (3) (see Section 2.2.7). When the shallow-area quota was filled, the vessels no longer had access to the *C. finmarchicus* concentration in grid cells shallower than 1000 m. This way, perfect fishing vessels could 'sense' where the optimal concentration of *C. finmarchicus* was and based on this knowledge decide whether to leave harbor or not.

Interactions. The IBM for fishing vessels was 2-way coupled to the *C. finmarchicus* model and enforced an extra grazing pressure at every time step. As the *C. finmarchicus* also served as food for pelagic fish, the fishing vessels were a direct competitor for these. The vessels did not directly interact with each other, but removal of *C. finmarchicus* due to fishing reduced the remaining abundance available for planktivorous fish and other fishing vessels.

Observations. For evaluating the performance of the fishing vessels, catch information (location and total catch) from 2 vessels (Arnøytind and Glomfjord) in 2015 from the Norwegian directorate of fisheries was used. The detailed catch data (longitude and latitude of the catches) were used in a cluster analysis, with the aim of defining individual fishing grounds and their mid points (longitude and latitude), which were needed as input to the model. This resulted in

the 10 fishing grounds guiding the fishing locations for the ordinary vessels (see Figs. 1 & 5). There were 199 stations included in the dataset, providing information on vessel, date, area, location, trawling time (h) and catch (kg). Detailed information on attributes of the vessels was collected from correspondence with CALANUS A/S (https://zooca.eu, accessed 19 October 2021), information online and based on information in Bastardie et al. (2014) (see Table 1 for details). Based on the towing time and catch given in the observations, the vessels operating in the *C. finmarchicus* fisheries currently have an average (±SD) catch per unit effort of 8.40 ± 4.99 t WW d^{-1}.

2.2.5. Initialization

The model was initiated on 1 January 1995 with 0, 10 or 60 individual fishing vessels. The initial harbors were predefined in the code, as were the levels of catch capacity, fuel usage etc. (see Table 1 for details). The harbors were located along the coast, in close proximity to both larger and smaller villages and/or cities, with the main aim of covering a larger part of the coast. The individuals were either ordinary or perfect vessels, with the perfect vessels being included to mimic a possible future improvement in fishing strategies. In the simulations with 10 individuals, they were all perfect or all ordinary, whereas in the simulations with 60 vessels, all were defined as perfect individuals. The fishing performed by the modelled fishing vessels mimicked the upper water column surface trawl fishery by assuming a trawl width of 7 m, covering a depth of up to 5 m, having 75% of the concentration (m^{-2}) of CIV–CVI copepods in the upper 100 m available for the catch:

$$\text{Catch} = \text{calfish} \cdot \text{trawlspeed} \cdot \text{gearsize} \cdot \text{gearnr} \cdot \text{trawltime} \cdot \text{vertfrac} \quad (1)$$

where calfish is the concentration (g WW m^{-2}) of CIV–CVI copepods in the upper 100 m (i.e. available to fishing), trawlspeed is the speed of the vessel when trawling, gearsize is 35 m^2, gearnr is the number of gears (2), and the time spent trawling (trawltime) was usually 24 h. Vertfrac is the vertical depth fraction (75%) in the upper 100 m where vessels had access to *C. finmarchicus*. This fraction ensured that there were *C. finmarchicus* available for the vessels, since *C. finmarchicus* fisheries operate from the surface down to 50 m depth (Fiskeridirektoratet 2016). However, it was among the more uncertain parameters (see Section 2.3).

2.2.6. Input

The fishing vessels got information on the daily spatial distribution of *C. finmarchicus* copepodite stage IV and V biomasses from the *C. finmarchicus* IBM module. The input was integrated over the upper 100 m, and the vessels had access to 75% of this biomass (vertfrac, Table 1).

2.2.7. Submodels

Movement. Two types of fishing vessels were implemented: ordinary vessels and perfect vessels (vessels with perfect knowledge of the *C. finmarchicus* distribution). The ordinary vessels would move towards predefined fishing grounds, while the perfect vessels would start fishing when it was economically feasible, potentially utilizing any area as a potential fishing ground. The approach for an ordinary fishing vessel to travel to and between fishing grounds was based on the logic loop defined in Bastardie et al. (2010), where the vessel considered at each time step whether the zooplankton concentration was high enough to initiate fishing at its current position, if it must return home to harbor due to fuel or storage capacity or move to another fishing ground (Fig. 3a). To avoid the fishing vessels crossing over land to get from A to B, at the same time as using the shortest path between 2 locations, we implemented Dijkstra's shortest path algorithm (Dijkstra 1959). This was only run initially (at the start of the model run), due to computational costs, as the model grid in total has about 21 000 grid cells. If a distance between location A and location B was too long for the vessel to travel in a day, the vessel would perform a stepwise movement over several days. When fishing at a location, the vessel was given a direction, which it would move toward when trawling. In these simulations, the given direction was always towards the closest one of the 3 surrounding fishing grounds.

Yield. The perfect vessel was not bounded by the predefined fishing grounds but had implicit knowledge of where and how much zooplankton it could find. It used yield as a measure for when to leave the harbor, given by:

$$\text{Yield} = \text{maxcarr} \cdot \text{catchprice} - \text{fuelcons} \cdot \text{fuelprice} \cdot \text{time} \quad (2)$$

where maxcarr was the maximum catch capacity (kg) of the vessel, catchprice the price of the catch (Norwegian kroner, NOK), fuelcons how much fuel the vessel consumed in total on the trip (l h^{-1}) and fuel-

price the price of fuel (NOK) (Table 1). Time (h) was the total time spent travelling from the respective harbor to the fishing ground, filling the vessel and then returning, given by:

$$\text{Time} = 2 \cdot \text{dist} / \text{speed} + \text{maxcarr} / (\text{calnode} \cdot \text{vertfrac} \cdot \text{trawlspeed} \cdot \text{gearsize} \cdot \text{nrgears}) \quad (3)$$

where dist was the distance (m) from harbor to fishing ground, speed was the steaming speed (m s^{-1}) of the vessel, calnode was the concentration of *C. finmarchicus* in a given grid cell (g WW m^{-2}), and trawlspeed was the speed (m s^{-1}) the vessel had while trawling. Thus, the logic loop was somewhat different from that of the ordinary vessel, with the perfect vessel staying in harbor until it was economically beneficial to go to the location giving the highest yield, fishing until full and then returning home (Fig. 3b).

2.3. Sensitivity analysis of factors in the fishing vessel module

Effective screening sensitivity of important factors in the perfect fishing vessel submodel was performed by applying a sensitivity analysis to Eq. (3). This was done by applying the Morris function in the 'sensitivity' package (Iooss et al. 2020) in R v.3.6.0 (R Core Team 2020). This follows the suggested sensitivity analysis of Morris (1991), but with the updates published in Campolongo et al. (2007). For each input, the Morris method calculates a number of incremental ratios, called Elementary Effects (EE) (Morris 1991, Campolongo et al. 2007). From these, the mean (m) and standard deviation (σ) are calculated. The updated Morris screening method provides μ, $\mu^\star$ and σ, where μ and $\mu^\star$ are the mean and the absolute mean respectively. They similarly represent the sensitivity of output to input due to all first and higher order effects, but only absolute values are used to calculate $\mu^\star$. σ is an indication of interactions and/or non-linearities. Only Eq. (3) was used as input to the screening method, due to the computational costs of the whole model system. Two model representations of Eq. (3) were implemented, with the first including all 11 parameters, while the second considered the concentration of *C. finmarchicus* and distance to the best fishing ground as constants. The reason for excluding concentration and distance to fishing ground was that these 2 factors were to a larger part independent of the processes within the fishing vessel module, and more dependent on factors included in e.g. the modules representing fish and *C. finmarchicus.* We performed 1000 replicates of the method, with 8 levels (space of parameter values, evenly distributed between and including minimum and maximum values) and 4 grid jumps (levels/2), as recommended in Morris (1991). The grid jump defines how many levels a parameter will change per step. The ranges of the parameters are provided in Table 2 and were based on the values applied in the fishing vessel module, applying ±50% variability.

2.4. Experimental set-up

The model was initiated on 1 January 1995. After a 4 yr spin-up repeating the forcing from 1995 letting the *C. finmarchicus* and NPZD model adjust from the initial field, the fishing vessel IBM started to fish *C. finmarchicus* and the fisheries were performed for the years 1995–1999. Four different simulations were done — (1) ref: reference simulations without the fishing vessels; (2) 10o: fishing was performed by 10 ordinary fishing vessels; (3) 10p: fishing was performed by 10 perfect fishing vessels; (4) 60p: fishing was performed by 60 perfect vessels.

All fishing vessels were allowed to operate throughout the whole year. The time step used by the fishing vessels is 1 d. The 10 vessel simulations were based on the number of vessels allowed to catch *C. finmarchicus* in 2020 (10 vessels in total), comparing the performance of the perfect and the ordinary vessels. The impact of the fisheries on regional biomass levels of *C. finmarchicus* was explored in 3 polygons (Lofoten north, Lofoten south and shelf edge; P1–P3 in Fig. 2). These polygons match areas with high fishing activity in the simulations. They are adapted from another end-to-end model covering the area (the Nordic and Barents Seas Atlantis model, Hansen et

Table 2. Parameters and their value range included in the Morris sensitivity tests. Names correspond to those in Eq. (3). NOK: Norwegian kroner

Parameter (unit)	Minimum value	Maximum value
Speed (ms^{-1})	1.5	4.5
Maxcarr (kg)	225 000	675 000
Trawl speed (ms^{-1})	0.25	0.75
Gearsize (m)	3.5	10.5
Nrgears (no.)	1	2
Catchprice (NOK)	5.5	16.5
Fuelcons (l h^{-1})	43.5	130.5
Fuelprice (NOK)	4	12
Vertfrac	0.375	1
Dist (m)	2.5×10^5	7.5×10^5
Calnode (g m^{-2})	5	15

al. 2019) and are constructed to be as homogeneous as possible with respect to bottom topography and water masses. All figures, except Fig. 1, were prepared using the ggplot2 package (Wickham 2016) in R (R Core Team 2020).

3. RESULTS

3.1. Sensitivity analysis

When applying the Morris screening method on the model including 11 parameters, among them concentration of *Calanus finmarchicus* and distance from fishing grounds, catch price turned out to have the largest impact, whereas the concentration of *C. finmarchicus* resulted in the highest variability (Fig. 4, green dots). Size and number of gears also had a rather large impact on the variability of the output. Speed and distance from the fishing ground were the 2 factors with the lowest impact on the results.

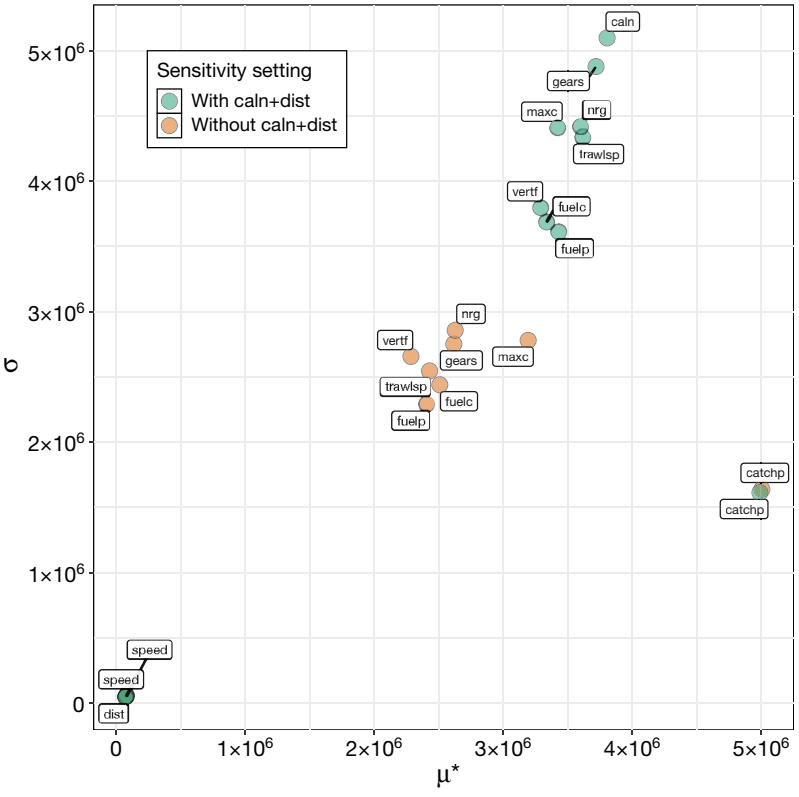

Fig. 4. Plots of σ versus μ* from the sensitivity analysis of Eq. (2), with concentration of *C. finmarchicus* and distance to best fishing ground held constant. Green dots include distance (dist) and concentration of *C. finmarchicus* (caln), while the orange dots exclude these 2 factors. Note that abbreviations vary from those in Table 1 to reduce amount of text in the figure. nrg: number of gears; gears: gear size; maxc: maximum catch capacity; vertf: available vertical fraction of *C. finmarchicus*; fuelp: fuel price; trawlsp: trawl speed; fuelc: fuel consumption

Applying the Morris method, excluding concentration of *Calanus finmarchicus* and the distance to the fishing ground, thereby reducing the number of factors to 9 (Figure 4, orange dots). Catch price had again the largest impact on the results, while speed did not have any influence. The 7 other factors had an intermediate and similar (to each other) impact on the results, with a somewhat higher variability than seen in the catch price. Exploring the 10 000 different combinations of parameters that the method gave as output, it was clear that simultaneously maximizing price and catch capacity gave the highest yield.

3.2. Simulations with ordinary vessels (Simulation 10o)

3.2.1. Catch

On average (±SD), the ordinary vessels in Simulation 10o caught 1827 ± 575 t WW yr^{-1}. The interannual differences were, however, large. The 2 first years represented the maximum and minimum average catches, with 978 t WW on average in 1995, increasing to 2493 t WW in 1996. Comparing the distribution of the *C. finmarchicus* biomass between these 2 years (Fig. 5) showed a lower biomass close to the coast, where the fishing grounds were located, in 1995 compared to 1996. In the 3 last years, the ordinary vessels caught on average 1889 t WW. Catch per unit effort (CPUE) was on average (±SD) 9.6 ± 1.8 t WW d^{-1} (Table 3). Maximum daily catch over all ordinary vessels and all years was 68.6 t.

3.2.2. Spatial and temporal differences

There was a significant and negative correlation ($r = -0.38$, $p < 0.01$) between total catch and the offshore catch fraction (catches outside the 1000 m isobath) for the 10o simulation. In general, the offshore catch fraction was low, averaging at 6.3% (Table 3). Only in 1997, 10 hotspots for fishing were identified. In the other years, the number varied between 8 (1995, 1996,

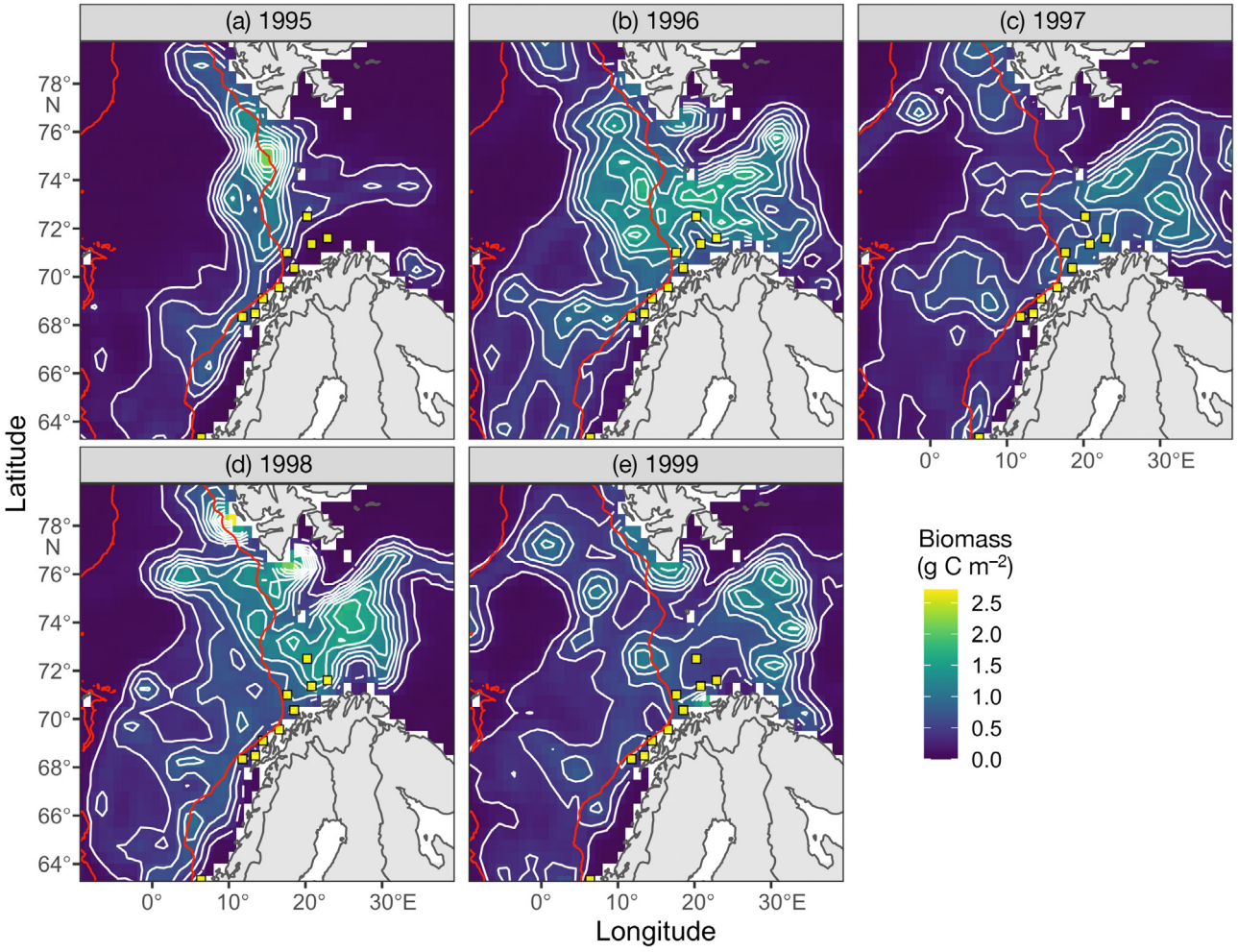

Fig. 5. Mean biomass (g C m^{-2}) of *C. finmarchicus* stages IV–VI in the upper 100 m for the main fishing period (10 Apr to 7 Sep) for the reference run (ref), in each of the 5 yr in the simulated period 1995–1999 (a–e respectively). Yellow squares: predefined fishing grounds. Red line: 1000 m depth contour

Table 3. Main characteristics and outcome of the simulations including fishing vessels. Average and minimum/maximum values (annual) are calculated over the whole simulation period (1995–1999). Simulations include no fishing vessels (ref), 10 ordinary vessels (10o), 10 perfect vessels (10p) and 60 perfect vessels (60p). WW: wet weight. For locations of P1, P2 and P3, see Fig. 2. NA is not applicable, as the Ref simulation does not include any vessels

Simulation name	Ref	10o	10p	60p
No. of ordinary vessels / no. of perfect vessels	0/0	10/0	0/10	0/60
Catch (1000 t)	NA	17	54	349
Average catch per vessel (1000 t yr^{-1})	NA	1.7	5.4	5.8
Minimum catch (1000 t yr^{-1})	NA	0.6	3.3	3.2
Maximum catch (1000 t yr^{-1})	NA	2.8	9.9	8.3
Average catch per unit effort (CPUE, t WW d^{-1})	NA	9.6	26.5	31.0
Offshore catch fraction (%)	NA	6.3	93.4	94.7
Lofoten north (P1, $\times 10^6$ t WW)	0.42 ± 0.18	0.36 ± 0.15	0.31 ± 0.21	0.28 ± 0.16
Lofoten south (P2, $\times 10^6$ t WW)	0.24 ± 0.05	0.27 ± 0.03	0.21 ± 0.03	0.28 ± 0.07
Shelf edge (P3, $\times 10^6$ t WW)	0.30 ± 0.09	0.32 ± 0.05	0.33 ± 0.07	0.31 ± 0.05

1999) and 9 (1998). The ordinary vessels had all their main activities within the area of the defined fishing grounds. For some years, the 2 southernmost hotspots (Fig. 6; green dots) had higher catches compared to the rest. Highest catches were typically found between Days 100 and 280, with some interan-

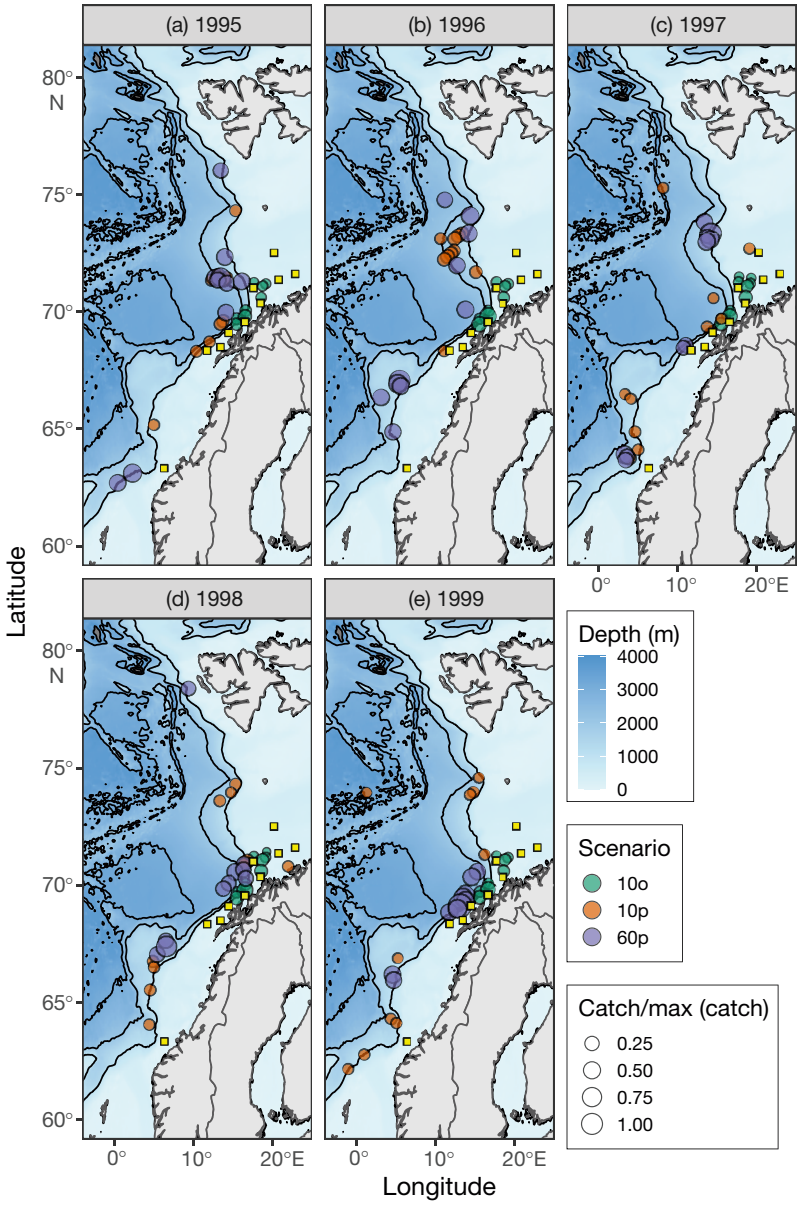

Fig. 6. Location of top 10 fishing grounds in simulation with 10 ordinary vessels (10o), 10 perfect vessels (10p) and 60 perfect vessels (60p) for 1995–1999 (a–e respectively). Circle size: fraction of catch caught at the specific location; yellow squares: location of the predefined fishing grounds utilized by the ordinary vessels. The shallowest contour line is at the 1000 m depth contour, indicating the restricted area (>1000 m). Maps were created using the marmap package in R (Pante & Simon-Bouhet 2013)

nual differences (Fig. 7). Before Day 100, there were generally too low concentrations of *C. finmarchicus* to initiate fishing. In 1996, a larger fraction of the catches was caught in late fall, due to persistently high *C. finmarchicus* values in the region around the predefined fishing grounds. Due to the low concentration of *C. finmarchicus* needed to initiate fishery activity (5 g WW m^{-2}), there were also incidents of low catches (<10 t WW d^{-1}) during the winter months (Fig. 7). On average, the ordinary vessels were fishing 189 d yr^{-1}. Fuel usage was on average ~474 000 l yr^{-1}, with a minimum of ~359 000 l yr^{-1} (in 1995) and a maximum of ~529 000 l yr^{-1} (in 1998).

3.3. Simulations including perfect vessels (Simulations 10p and 60p)

3.3.1. Catch

The perfect vessels in 10p caught on average (±SD) 5508 ± 1794 t WW yr^{-1}. The maximum catch occurred in 1996 (7867 t WW per vessel), and the minimum in 1999 (3948 t WW per vessel). CPUE was 27 ± 6.5 t WW d^{-1} in 10p. Introducing 60 perfect vessels led to an increase in the average catches, to 5826 t WW per vessel. CPUE for the 60 vessels was 32 ± 4.3 t WW d^{-1}. The lowest average catch per vessel occurred in 1997 (4457 t WW per vessel), while the maximum occurred in 1999 (7186 t WW per vessel). The maximum catch caught in 1 d, for all perfect vessels and all years in Simulation 10p was 147.5 t WW, while it was 162.9 t WW in Simulation 60p.

3.3.2. Spatial and temporal differences

The correlation between the total catches and the offshore catch fraction in 10p was lower ($r = 0.36$, $p < 0.02$) than for the ordinary vessels. The offshore catch fraction was high (>92%) but with a large variability among the vessels, from 76 to 100%. In 60p, the offshore catch fraction was even higher (>99%) than in 10p. While there was some overlap among the top 10 fishing grounds for 10p and 60p, the simulations largely identified different hotspots for fishing *C. finmarchicus* (Fig. 6). Except for a few hotspots (10p, orange dots in Fig. 6; 1997 and 1999), they were all located along the shelf edge. The period with the largest catches was around Day 175 (Fig. 7), with low or no catches before Day 100.

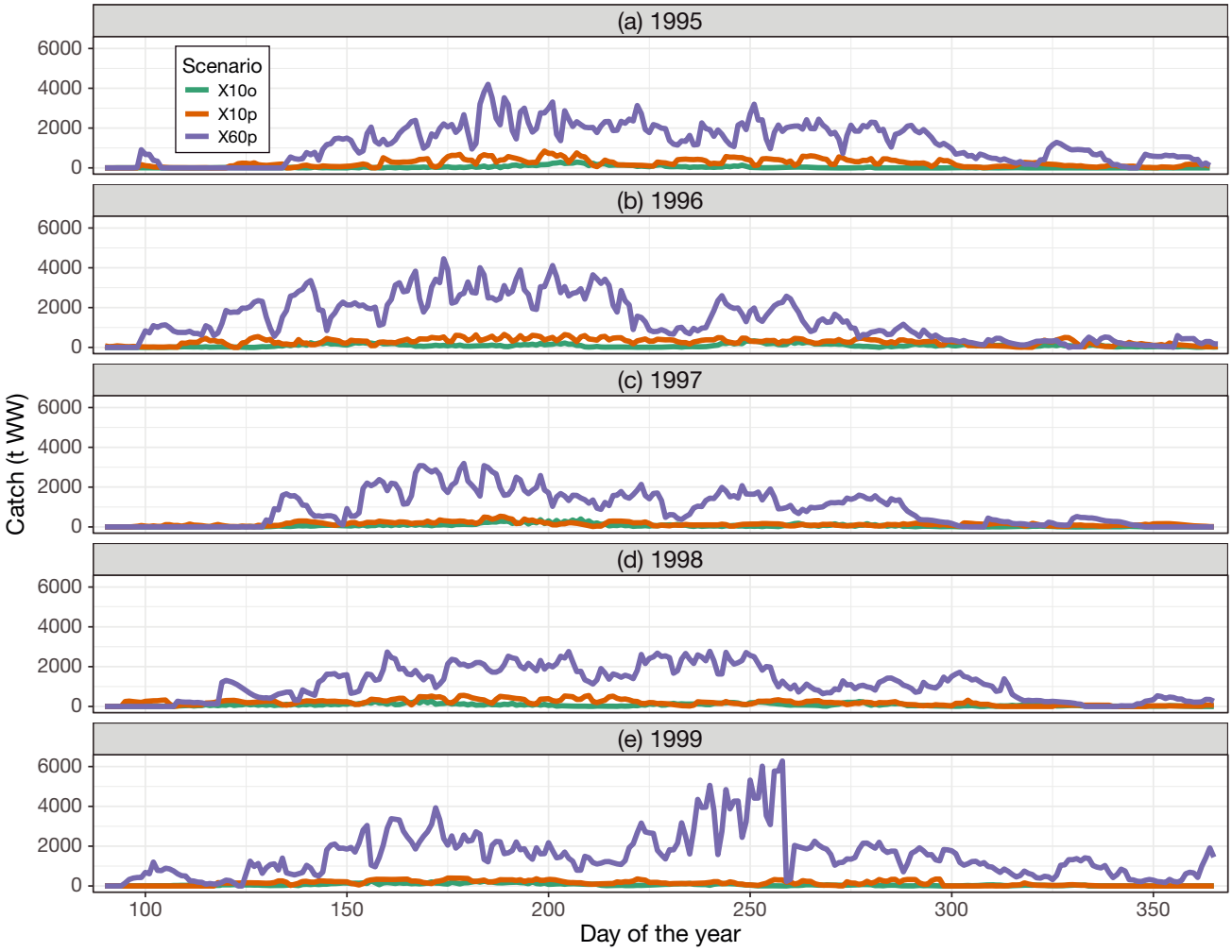

Fig. 7. Average harvest pattern for the 3 simulations for the 5 yr of the simulation (1995–1999, a–e respectively). The ordinary vessels (10o) experienced a larger variability, compared to the perfect vessels (10p and 60p). Catches before Day 100 were very low and are not shown

From Day 250, the catches per day declined. On average, the perfect vessels fished 202 and 183 d yr^{-1} for Simulations 10p and 60p respectively. The fuel usage was on average 477 000 l yr^{-1} for Simulation 10p, with a minimum of 437 000 l yr^{-1} (in 1999) and a maximum of 548 000 l yr^{-1} (in 1996). Including 60 perfect vessels decreased the average fuel usage to 432 000 l yr^{-1}, with a maximum of 498 000 l yr^{-1} (in 1999) and a minimum of 400 000 l yr^{-1} (in 1995).

3.4. Ecosystem effects of *Calanus finmarchicus* fisheries

The differences in summer biomass of *C. finmarchicus* between the reference run (ref) and each of the simulations including fishing vessels (10o, 10p, 60p) ranged from 0–9% (Table 4) and were either positive (increase in *C. finmarchicus* biomass due to fishing) or negative (decrease in *C. finmarchicus* biomass due to fishing). None of the simulations was always positive or negative, and only in 1997 showed

Table 4. *Calanus finmarchicus* biomass in summer in the reference run (ref) and difference in biomass between reference run and each simulation including vessels (10o: 10 ordinary vessels, 10p: 10 perfect vessels, 60p: 60 perfect vessels)

Year	Biomass ($\times 10^7$ t WW)	Difference to ref (%)		
	Ref	10o	10p	60p
1995	7.65	−6.3	0.6	1.6
1996	1.18	−0.6	−4.8	5.2
1997	1.13	4.7	0.5	5.4
1998	1.31	−8.9	−3.1	−0.8
1999	1.22	−7.4	−7.1	2.3

Table 5. Norwegian spring spawning herring biomass in the summer in the reference run (ref), and difference between reference and each simulation including vessels (see Table 4 for definitions)

Year	Biomass ($\times 10^6$ t WW)	Difference to ref (%)		
	Ref	10o	10p	60p
1995	7.4	0.2	0.2	0.2
1996	8.7	−1	0.7	−1.8
1997	10.0	−3.4	1	−2
1998	11.9	−3.9	4.1	−0.1
1999	14.1	−4.1	5.6	0.4

a consistent positive difference, while in 1998 a consistent negative difference was present across the simulations. Exploring effects on a local scale revealed that for the Lofoten north polygon (Fig. 2), a consistent negative effect was found in Simulation 60p. The difference between the reference simulation without fishing and the simulation with 60 perfect vessels varied from −7 to −62% for the summer biomass of *C. finmarchicus*, depending on the year (Table 3). Neither of the 2 other polygons we explored showed any such patterns (Table 3). Comparing the NSS herring summer biomass between the reference run and 10o, 10p and 60p revealed small differences between −4.1 and 5.6% (Table 5). The time series was too short to be certain whether what seemed like an increasing negative difference between the reference run and the fish biomass in the simulation including ordinary vessels only (10o), was a significant pattern. Exploring the biomass of the different age classes of simulated herring revealed that there was a negative impact in the simulation including only ordinary vessels (10o) from the second year onwards (data not shown). This difference from the reference run leveled out at 3% toward the end of the simulation. The first age class (up to 1 yr old) in the simulation including 10 perfect vessels (10p) showed a positive response (which leveled out at about 8% towards the end of the simulation) compared to the reference run. The first age class of herring in the simulation including 60 perfect vessels experienced a low positive difference (<5%) throughout most of the simulation period compared to the reference run.

4. DISCUSSION

In this study, an IBM for fishing vessels was used to explore vessel behavior, catches, performance and ecosystem impacts of harvesting *Calanus finmarchicus*, the main secondary producer in the Norwegian Sea. The horizontal resolution of the model was relatively coarse, with a grid resolution of 20 × 20 km, due to availability of forcing files. The simulations with 10 perfect or 10 ordinary vessels reflected the number of licenses provided by the Norwegian Fisheries Directorate (10 licenses in total in 2020). The CPUE varied significantly between the ordinary and the perfect vessels, being roughly 3 times higher for the latter. In the simulation with 60 perfect vessels, the aim was to explore potential effects of catching at least the full quota of *C. finmarchicus* (253 000 t). Our results show small ecosystem effects of harvesting *C. finmarchicus*, even when more than 130% of the current quota was harvested. Although an overall ecosystem effect could not be found, a local decline in the summer *C. finmarchicus* biomass was evident in the Lofoten north polygon in the simulation with 60 perfect vessels.

4.1. Model performance and sensitivity

Zooplankton monitoring is challenging due to patchiness in time and space and the vast size of the study area, which makes synoptic sampling impossible and gross estimates of biomass from observations difficult (Hjøllo et al. 2021 in this Theme Section). Focusing on the year 1997, Hjøllo et al. (2012) found modelled *C. finmarchicus* spatial distribution, production and biomass to represent observations reasonably well, although the timing of the spring bloom was somewhat later than in the observations. The model also gave an elevated autumn biomass. The high autumn biomass values are related to the lack of knowledge of the controlling mechanisms for starting the diapause (Hjøllo et al. 2021, Gao et al. 2021). The elevated autumn-levels impact the fishing patterns of both the perfect and the ordinary vessels by introducing catches in late autumn and winter (Fig. 7). However, it should be noted that there are few observations for this time of the year, and peak abundances until October have been seen in continuous plankton recorder (CPR) data in the central Norwegian Sea (Strand et al. 2020).

The sensitivity analysis identified some of the fishing vessel parameters as being more important than others. In the version of the model applied in these simulations, the vessels had access to 75% of the *C. finmarchicus* in the upper 100 m, covering more than ~50 m depth that are currently exploited by the fisheries (Fiskeridirektoratet 2016). However, the frac-

tion of *C. finmarchicus* in the upper 100 m available for the fishery (vertfrac, Table 1) was not among the most sensitive parameters identified in the sensitivity analysis, although it doubtlessly will have a direct impact on the total catches. Nevertheless, the known patchiness in zooplankton fields and the gear size are issues that might have a large impact on the catchability. Another source of uncertainty is the spatial resolution of the model grid, which translated into the fishing vessels fishing on the average concentrations of *C. finmarchicus* within an area of 400 km^2. With increasing resolution, the modelled *C. finmarchicus* concentrations would likely be more patchily distributed, and thus fishing vessels could potentially locate and exploit these higher concentrations, resulting in higher total catches and CPUE. The CPUE of ordinary vessels, with an average of 9.6 t WW d^{-1}, was higher than in the observations at 8.4 t WW d^{-1}. The higher efficiency in the ordinary vessels potentially emerges from a higher catchability, but also from not taking weather conditions and other restrictions on the fisheries into account.

Maximum catch capacity and the price of the catch were important for the total yield of the vessels, while the number and size of gear played an important role in the variability of the results (Fig. 4). Catch capacity and price of catch are not independent, as higher catches following an increase in catch capacity in the vessels potentially will influence the price of the catch. In contrast to the fisheries explored in Bastardie et al. (2014), this is a completely new fishery, with little data except that of the trial fishery, which probably is not representative for a large-scale fishery for *C. finmarchicus*. In this respect, implementing the perfect vessels was an attempt to introduce a more developed fishery with better knowledge on stock distribution. Adding an even more refined human dimension at this stage would possibly only introduce a set of uncertainties which could neither be tuned nor evaluated. There are multiple possibilities for refining the fishing vessels. However, this procedure also depends upon more observations and would greatly benefit from a transdisciplinary approach (Essington et al. 2017, Burgess et al. 2020). This was out of the scope for this project but should be taken into consideration in future developments of the model.

4.2. Differences between current (ordinary) and potential future (perfect) fishing vessels

roducing perfect vessels, with intrinsic knowledge of the modelled *C. finmarchicus* spatial and temporal distribution, can be seen to mimic a possible future in-depth knowledge of the *C. finmarchicus* distribution from a combination of models and observations. Also, decreasing the uncertainty around the fishers' behavior by letting the vessel have perfect knowledge reduces the effect of fishing vessel model limitations.

Large spatial differences were found between the predefined fishing grounds and the top 10 fishing grounds emerging from the perfect vessels. Few of the catches of the perfect vessels were found at or near the catch-diary-defined fishing grounds (Fig. 6). This pattern emerged partly from the area restrictions for the perfect vessels, as only 3000 t were allowed in areas shallower than 1000 m. It could also potentially be due to lack of details in the simulated *C. finmarchicus* distribution or because of a spatial mismatch between simulated *C. finmarchicus* fields based on the simulated years and the actual *C. finmarchicus* distribution in recent years. However, this is a relatively immature fishery, and less is known about the hotspots of *C. finmarchicus* compared to the more established fishing grounds of commercial species like mackerel or NSS herring. The newly identified fishing grounds should therefore be seen as potential fishing grounds within reach of a commercial fishery. The original fishing grounds are located relatively close to shore, all with a depth <1000 m. This will be problematic, as the vast majority of the quota has to be caught offshore (Broms et al. 2016, www.regjeringen.no/no/dokumenter/forskrift-om-regulering-av-hosting-av-rodate-i-2019/id2632216/, accessed 19 October 2021). Restricting the vessels to be allowed only 3000 t within the 1000 m depth contour resulted in offshore catch fractions for the perfect vessels of >93% (Table 3). Furthermore, technological developments in large scale observing systems such as satellites (Basedow et al. 2019) may hold a key to future harvesting by ordinary vessels being more along the lines of our modelled perfect vessels.

The significant difference in CPUE between the ordinary and the perfect vessels points to the advantage of knowledge on where the *C. finmarchicus* concentrations are large enough to support an economically beneficial fishery. The activity level for both ordinary and perfect vessels was about the same (~190 d yr^{-1}), but the perfect vessels realized a catch 3 times higher compared to the ordinary vessels during this activity period. At the same time, the two vessel types used about the same level of fuel. Hence, the total costs of the fishery were significantly higher for the ordinary vessels compared

to the perfect vessels. The high fuel usage for the simulations including 10 or 60 perfect vessels was explained by the shift of the fishing grounds further offshore.

4.3. Ecosystem effects of harvesting *C. finmarchicus*

Consequences of increased fishing on the more productive lower trophic levels of the ecosystem have been discussed in numerous papers (see e.g. Smith et al. 2011). A good example is krill, which has been harvested in the Southern Ocean for decades, with ongoing debates regarding its impact on the ecosystem (see e.g. Watters et al. 2020). Inclusion of IBMs for fish allowed us to explore ecosystem effects of the *C. finmarchicus* catch and the development of a viable fishery. Using 10 vessels, either ordinary or perfect, resulted in total annual catches that were far from the full quota (17 000 and 54 000 t respectively, Table 3). Compared to the total *C. finmarchicus* standing stock biomass, these catches account for only 0.02 and 0.05% respectively. Hence, no effects on either herring biomass or *C. finmarcus* biomass were evident in the model simulations. Introducing 60 perfect vessels increased the total catch to 349 000 t over the simulation period (Table 3), adding up to 0.31% of the total *C. finmarchicus* biomass. In this simulation, small variations in the distribution and concentration of *C. finmarchicus* summer biomass between the reference runs and the simulation with 60 perfect vessels could be found. However, comparing the total biomass between the reference run and 60 perfect vessels did not show any consistent differences (Table 4). Increasing levels of *C. finmarchicus* biomass when introducing fishing (Table 4) was due to density-dependent effects, where removal of biomass caused better living conditions for the remaining individuals.

The small negative impact on the herring biomass arising in the simulation including 10 ordinary vessels indicates that harvest at this level (17 000 t annual catch) within a relatively small area, only at shallow depths, might introduce ecosystem effects. The negative response was first evident in the young fish (<1 yr old) and moved through the cohorts. The low positive responses in herring biomass seen in the simulations including the perfect vessels decreased with increasing harvest levels, suggesting that positive density-dependent effects can be eliminated when approaching (or as in this case exceeding) the total allowed catch. The decrease in summer *C. finmarchicus* biomass in the Lofoten north polygon seen in the simulation with the 60 perfect vessels might also have an impact on other marine life that depends on mesozooplankton. Zooplankton are not stationary and will be advected out of and into an area following the currents. Future management plans should evaluate how to avoid harvesting the majority of catches within a small area, if or when the commercial catch is approaching the allowed quota. However, the lack of consistent, negative effects in the simulation with the 60 perfect vessels indicated that the precautionary catch level and the area restrictions defined in the management plans (Fiskeridirektoratet 2016) are reasonable.

4.4. Model refinements

Given the level of uncertainty and number of unknowns in a new fishery such as the *C. finmarchicus* fishery, we consider this model development to be the first step towards a more sophisticated IBM for fishing vessels. Currently, the model does not take into account weather or weekdays, nor does it consider work permits and work regulations. Considering such factors would probably act as a counter-effect for the late autumn and winter catches seen in the simulated harvest patterns (Fig. 7). To decrease the number of active days for the ordinary vessels, further knowledge of what the threshold for initiating fishing activity should be compared to the current threshold of 5 g WW m^{-2} (fishlimit, Table 1). The equations determining the total yield are simple and could be made more nuanced, taking into consideration additional costs and benefits as well as more information on how the vessels/fishermen make their decisions. However, all these refinements rely on more and better information from a newly initiated fishery, not only forn the parameters, but also for validating the model results.

In terms of biology, there were also simplifications, e.g. the number of predators on *C. finmarchicus*, fisheries-induced mortality at younger life stages of *C. finmarchicus* and additional mortality on other ecosystem components due to bycatch. *C. finmarchicus* copepodite stages younger than the main target stages will in principle slip through the trawl meshes due to their smaller size. However, a certain amount will probably be caught in the trawl as bycatch. In addition, individuals that go through the trawl meshes may be injured and die. Quantitative measurements from the *C. finmarchicus* fisheries concern-

ing mortality due to bycatch of younger copepodite stages or trawl escape are lacking; however, experiences from the Antarctic krill fisheries suggest that mortality of krill escaping the trawl nets is relatively low (Krafft et al. 2016). We therefore recommend that the ecosystem effects of exploiting hotspots of *C. finmarchicus*, both outside of known spawning grounds for fish and in the shallow coastal areas, should be further explored.

5. CONCLUSIONS

Fishing *Calanus finmarchicus* in the Norwegian Sea has large potential, with high yields. The standing stock is large (Hjøllo et al. 2012), but less is known about offshore hotspots that can be used as fishing grounds. This knowledge is important due to the split of the quota between the 3000 t allowed inshore compared to the 254 000 t allowed outside the 1000 m depth contour.

Neither the 10 ordinary nor the 10 perfect vessels applied in the model were able to catch the total quota. Increasing the number of vessels to 60 with the current gear, perfect weather and knowledge about the hotspots, the total catch was 349 000 t, almost 40% above the current quota. Although there are numerous simplifications in the module developed and model system applied, the model system still reflects the difficulties that the fishers face in this kind of fishery. On the other hand, it supports the possibility of a sustainable *C. finmarchicus* fis hern the Norwegian Sea, as the ecosystem impacts on herring and on the *C. finmarchicus* biomass in the simulated system were low.

So far, very few ecosystem models have been used in fisheries management (Lehuta et al. 2016, Skern-Mauritzen et al. 2016). NORWECOM.E2E was part of the preparation of the *C. finmarchicus* management report (Broms et al. 2016), but improvements of fish IBMs and the implementation of fishing vessel IBMs should further strengthen the use of ecosystem models when changes in fisheries management are considered. The module presented here could potentially be further developed to explore effects of bycatch and fishery-induced mortality on other life stages than those targeted. More mature ecosystem models of this kind could also inform managers about the consequences of fishing at hotspots not previously harvested. Given the uncertainty that comes with large end-to-end ecosystem models (Fulton 2010, Link et al. 2012, Lehuta et al. 2016), models would have to be used alongside other tools. Still, the present study suggests a future use of ecosystem models that can be increasingly helpful for both managers and fishers.

Acknowledgements. C.H., E.S., M.D.S. and S.S.H. acknowledge support from the project HArvesting LOwer trophic levels (project number 234341), funded by The Research Council of Norway. C.H. acknowledges support from the Institute of Marine Research Strategic Project 'Reduced Uncertainty in Stock Assessment' (2016–2020), project number 3680_14809. C.H. and M.D.S. also acknowledge support from the European Union's Horizon 2020 Research and Innovation programme under grant agreement no. 727890 (INTAROS). C.B. acknowledges support from the Institute of Marine Research Strategic Project 'Sustainable harvesting in the Norwegian Sea and adjacent ecosystems' (project number 299554), funded by The Research Council of Norway. Thanks to Ina Nilsen for kindly letting us use the silhouettes of phytoplankton, zooplankton and herring in Fig. 1. Finally, we appreciate the valuable feedback we got from 3 anonymous reviewers on an earlier version of the manuscript.

LITERATURE CITED

Bachiller E, Utne KR, Jansen T, Huse G (2018) Bioenergetics modeling of the annual consumption of zooplankton by pelagic fish feeding in the Northeast Atlantic. PLOS ONE 13:e0190345

Basedow SL, McKee D, Lefering I, Gislason A and others (2019) Remote sensing of zooplankton swarms. Sci Rep 9: 686

Bastardie F, Nielsen JR, Andersen BS, Eigaard OR (2010) Effects of fishing effort allocation scenarios on energy efficiency and profitability: an individual-based model applied to Danish fisheries. Fish Res 106:501–516

Bastardie F, Nielsen JR, Miethe T (2014) DISPLACE: a dynamic, individual-based model for spatial fishing planning and effort displacement — integrating underlying fish population models. Can J Fish Aquat Sci 71: 366–386

Broms C, Melle W (2007) Seasonal development of *Calanus finmarchicus* in relation to phytoplankton bloom dynamics in the Norwegian Sea. Deep Sea Res II 54:2760–2775

Broms C, Strand E, Utne KR, Hjøllo S, Sundby S, Melle W (2016) Vitenskapelig bakgrunnsmateriale for forvaltningsplan for raudåte. Fisken og Havet Rapport 8-2016 (in Norwegian with English Abstract). https://imr.brage.unit.no/imr-xmlui/handle/11250/2440945

Budgell WP (2005) Numerical simulation of ice-ocean variability in the Barents Sea region. Ocean Dyn 55:370–387

Burgess MG, Carrella E, Drexler M, Axtell RL and others (2020) Opportunities for agent-based modelling in human dimensions of fisheries. Fish Fish 21:570–587

Campolongo F, Cariboni J, Saltelli A (2007) An effective screening design for sensitivity analysis of large models. Environ Model Softw 22:1509–1518

Dalpadado P, Arrigo KR, Hjøllo SS, Rey F and others (2014) Productivity in the Barents Sea — response to recent climate variability. PLOS ONE 9:e95273

Dijkstra EW (1959) A note on two problems in connexion with graphs. Numer Math 1:269–271

Essington TE, Ciannelli L, Heppell SS, Levin PS and others (2017) Empiricism and modeling for marine fisheries: advancing an interdisciplinary science. Ecosystems 20: 237–244

FAO (Food and Agriculture Organization of the United Nations) (2020) FAO Yearbook. Fishery and aquaculture statistics 2018. FAO, Rome

Fiskeridirektoratet (2016) Forvaltningsplan for raudåte. Fiskeridirektoratet, Tech rep. www.fiskeridir.no/Yrkesfiske/Dokumenter/Rapporter/2016/Forvaltningsplan-for-raudaate (accessed 19 October 2021)

Fulton EA (2010) Approaches to end-to-end ecosystem models. J Mar Syst 81:171–183

Gao S, Hjøllo SS, Falkenhaug T, Strand, E, Edwards M, Skogen MD (2021) Overwintering distribution, inflow patterns and sustainability of *Calanus finmarchicus* in the North Sea. Prog Oceanogr 194:102567

Garcia SM, Kolding J, Rice J, Rochet MJ and others (2012) Reconsidering the consequences of selective fisheries. Science 335:1045–1047

Grimm V, Berger U, Bastiansen F, Eliassen S and others (2006) A standard protocol for describing individual-based and agent-based models. Ecol Modell 198: 115–126

Hansen C, Nash RDM, Drinkwater KF, Hjøllo SS (2019) Management scenarios under climate change — a study of the Nordic and Barents Seas. Front Mar Sci 6:668

Hjøllo SS, Huse G, Skogen MD, Melle W (2012) Modelling secondary production in the Norwegian Sea with a fully coupled physical/primary production/individual-based *Calanus finmarchicus* model system. Mar Biol Res 8: 508–526

Hjøllo SS, Hansen C, Skogen MD (2021) Assessing the importance of zooplankton sampling patterns with an ecosystem model. Mar Ecol Prog Ser 680:163–176

Huse G, Strand E, Giske J (1999) Implementing behaviour in individual-based models using neural networks and genetic algorithms. Evol Ecol 13:469–483

Huse G, Melle W, Skogen MD, Hjøllo SS, Svendsen E, Budgell WP (2018) Modeling emergent life histories of copepods. Front Ecol Evol 6:23

Iooss B, Da Veiga S, Janon A, Pujol G (2020) sensitivity: global sensitivity analysis of model outputs. R package version 1.23.0. https://CRAN.R-project.org/package=sensitivity

Krafft BA, Krag LA, Engås A, Nordrum S, Bruheim I, Herrmann B (2016) Quantifing the escape mortality of trawl caught Antarctic krill (*Euphausia superba*). PLOS ONE 11:e0162311

Langøy H, Nøttestad L, Skaret G, Broms C, Fernö A (2012) Overlap in distribution and diets of Atlantic mackerel (*Scomber scombrus*), Norwegian spring-spawning herring (*Clupea harengus*) and blue whiting (*Micromesistius poutassou*) in the Norwegian Sea during late summer. Mar Biol Res 8:442–460

Lehuta S, Girardin R, Mahévas S, Travers-Trolet M, Vermard Y (2016) Reconciling complex system models and fisheries advice: practical examples and leads. Aquat Living Resour 29:208

Lien VS, Budgell PW, Ådlandsvik B, Svendsen E (2006) Validating results from the model ROMS (Regional Ocean Modelling System), with respect to volume transports and heat fluxes in the Nordic Seas. Fisken og Havet, technical report, 2006-2

Link JS, Ihde TF, Harvey CJ, Gaichas SK and others (2012) Dealing with uncertainty in ecosystem models: the paradox of use for living marine resource management. Prog Oceanogr 102:102–114

Melle W, Ellertsen B, Skjoldal HR (2004) Zooplankton: the link to higher trophic levels. In: Skjoldal HR (ed) The Norwegian Sea ecosystem. Tapir Academic Press, Trondheim, p 137–202

Misund OA, Vilhjálmsson H, Jákupsstovu SH í, Røttingen I and others (1998) Distribution, migration and abundance of Norwegian spring spawning herring in relation to the temperature and zooplankton biomass in the Norwegian Sea as recorded by coordinated surveys in spring and summer 1996. Sarsia 83:117–127

Morris MD (1991) Factorial sampling plans for preliminary computational experiments. Technometrics 33:161–174

Olafsdottir AH, Utne KR, Jacobsen JA, Jansen T and others (2019) Geographical expansion of Northeast Atlantic mackerel (*Scomber scombrus*) in the Nordic Seas from 2007 to 2016 was primarily driven by stock size and constrained by low temperatures. Deep Sea Res II 159: 152–168

Pante E, Simon-Bouhet B (2013) marmap: a package for importing, plotting and analyzing bathymetric and topographic data in R. PLOS ONE 8:e73051

Prokopchuk I, Sentyabov E (2006) Diets of herring, mackerel, and blue whiting in the Norwegian Sea in relation to *Calanus finmarchicus* distribution and temperature conditions. ICES J Mar Sci 63:117–127

R Core Team (2020) R: a language and environment for statistical computing. R Foundation for Statistical Computing, Vienna. www.R-project.org

Scheffer M, Baveco JM, DeAngelis DL, Rose KA, van Nes EH (1995) Super-individuals a simple solution for modelling large populations on an individual basis. Ecol Modell 80:161–170

Shchepetkin AF, McWilliams JC (2005) The regional oceanic modeling system (ROMS): a split-explicit, free-surface, topography-following-coordinate oceanic model. Ocean Model 9:347–404

Skaret G, Dalpadado P, Hjøllo SS, Skogen MD, Strand E (2014) *Calanus finmarchicus* abundance, production and population dynamics in the Barents Sea in a future climate. Prog Oceanogr 125:26–39

Skern-Mauritzen M, Ottersen G, Handegard NO, Huse G, Dingsør GE, Stenseth NC, Kjesbu OS (2016) Ecosystem processes are rarely included in tactical fisheries management. Fish Fish 17:165–175

Skjoldal HR, Saetre R, Fernö A, Misund OA, Dommasnes A (2004) The Norwegian Sea ecosystem. Tapir Academic Press, Trondheim

Skogen MD, Svendsen E, Berntsen J, Aksnes D, Ulvestad KB (1995) Modeling the primary production in the North Sea using a coupled 3-dimensional physical, chemical, biological ocean model. Estuar Coast Shelf Sci 41: 545–565

Smith ADM, Brown CJ, Bulman CM, Fulton EA and others (2011) Impacts of fishing low-trophic level species on marine ecosystems. Science 333:1147–1150

Strand E, Bagøien E, Edwards M, Broms C, Klevjer T (2020) Spatial distributions and seasonality of four *Calanus* species in the Northeast Atlantic. Prog Oceanogr 185: 102344

Utne KR, Huse G (2012) Estimating the horizontal and temporal overlap of pelagic fish distribution in the Norwegian Sea using individual-based modelling. Mar Biol Res 8:548–567

Utne KR, Hjøllo SS, Huse G, Skogen M (2012) Estimating the consumption of *Calanus finmarchicus* by planktivorous fish in the Norwegian Sea using a fully coupled 3D model system. Mar Biol Res 8:527–547

Vihtakari M (2021) ggOceanMaps: plot data on oceanographic maps using 'ggplot2'. R package version 1.1. https://CRAN.R-project.org/package=ggOceanMaps

Watters GM, Hinke JT, Reiss CS (2020) Long-term observations from Antarctica demonstrate that mismatched scales of fisheries management and predator–prey interaction lead to erroneous conclusions about precaution. Sci Rep 10:2314

Wickham H (2016) ggplot2: elegant graphics for data analysis, 2nd edn. Springer, New York, NY

Zhou S, Kolding J, Garcia SM, Plank MJ and others (2019) Balanced harvest: concepts, policies, evidence, and management implications. Rev Fish Biol Fish 29: 711–733

Editorial responsibility: Aaron Adamack (Guest Editor), St. John's, Newfoundland and Labrador, Canada
Reviewed by: T. Russo and 2 anonymous referees

Submitted: January 8, 2021;
Accepted: October 20, 2021
Proofs received from author(s): November 27, 2021